Nuclear Effects at HERMES

V. Muccifora
INFN, Laboratori Nazionali di Frascati, Italy
On behalf of the HERMES collaboration

Abstract

Nuclear effects have been studied at HERMES in inclusive, semi-inclusive and exclusive reactions on ^2H, ^3He and ^{14}N unpolarized targets.

Inclusive inelastic scattering measurements on nuclear targets have provided fundamental new insights into the structure of the nucleon and how it is affected by the nuclear medium. Moreover, the effect of the nuclear medium on hadron production and quark propagation processes in deep inelastic scattering has been studied.

1 Introduction

Deep inelastic lepton-nucleon scattering (DIS) plays an essential role in the development of present understanding of the sub-structure of hadrons.

The interaction of the lepton with the constituents of the nucleon can be studied by detecting the scattered lepton only, this is known as inclusive DIS. In addition the formed final hadrons can be studied in semi-inclusive DIS (SIDIS), involving the detection of part of the hadronic final state, or in exclusive DIS where the complete identification of the final state is performed.

In DIS the lepton interacts with the constituents of the nucleon by the exchange of a virtual photon. The energy transfer (ν) of the virtual photon to the target nucleon (of mass M), and the four-momentum transfer (Q^2) completely constraint the kinematic of an inclusive event. They are related to the energy of the incident (E) and scattered lepton (E') and to the scattering angle (θ) in the laboratory frame:

$$\nu = E - E', \qquad Q^2 = 4EE' sin^2(\theta/2).$$

Three dimensionless variables x, y and z are used to describe the kinematics of DIS and SIDIS processes:

$$x = Q^2/2M\nu, \quad y = \nu/E', \quad z = E_h/\nu;$$

where x is the nucleon momentum fraction of the struck quark, y is the energy fraction of the virtual photon and z is the fraction of the photon energy ν transfered to hadron h.

The kinematics of the HERMES experiment are well-matched with the typical nuclear length scales. Hence, measurements that want to exploit the nuclear medium, and thus want to maximize its influence, can be performed at HERMES.

Nuclear effects have been studied at HERMES in inclusive, semi-inclusive and exclusive reactions on ^2H, ^3He and ^{14}N unpolarized targets.

2 The HERMES experiment

The HERMES (HERA MEasurement of Spin) experiment [1] is located at DESY and uses the 27.5 GeV HERA electron/positron beam which is longitudinally polarized in the HERMES region with an average polarization of $\sim 55\%$.

HERMES is a forward spectrometer (see fig.1) with a dipole magnet providing an integrated field of 1.3 Tm. The spectrometer consists of two identical detector systems, upper and lower, with polar angle acceptance between 40 mrad and 220 mrad. Tracking is performed by several sets of position sensitive detectors before, inside and after the dipole magnet. Particle identification is accomplished using a lead glass calorimeter, a preshower, a six-module transition detector and a $C_4F_{10}/N_2(70 : 30)$ gas threshold Čerenkov counter. The threshold Čerenkov detector has been replaced in 1998 with a dual-radiator ring-imaging Čerenkov to identify pions, kaons and protons over nearly to the entire momentum acceptance of the spectrometer.

The experiment has been designed to investigate the spin structure of the nucleon by using polarised internal gas targets. In addition unpolarised measurements on nuclear targets, addressed to the study of the nuclear medium effects, have been performed. These unpolarised data are usually collected in short time periods of a few days or a week at relatively high luminosity (L) ($L \sim 10^{33} nucleons/cm^2s$). Results from these measurements will be reported in the next sections.

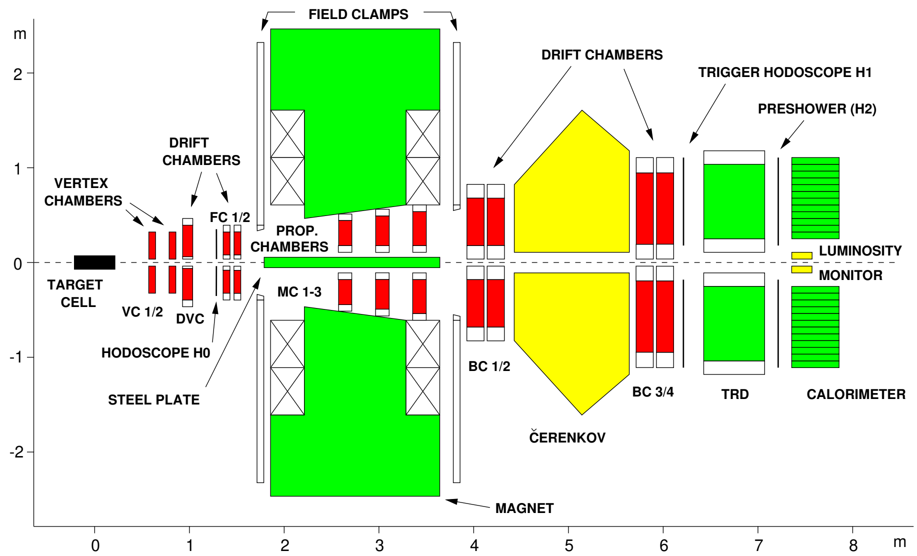

Figure 1: Longitudinal view of the HERMES spectrometer.

3 Inclusive Measurements

The DIS double-differential cross section per nucleon from an unpolarised target can be written in terms of the cross section for the absorption of transversly (σ_T) and longitudinal (σ_L) polarized virtual photon:

$$\frac{d^2\sigma}{dxdQ^2} = \Gamma(\sigma_T + \epsilon\sigma_L),$$

where $\Gamma = \frac{\alpha(\nu - Q^2/2M)E'}{2\pi^2 Q^2 E(1-\epsilon)}$ is the virtual photon flux and $\epsilon = \frac{4(1-y)-Q^2/E^2}{4(1-y)+2y^2+Q^2/E^2}$ is the virtual photon polarization parameter.

This cross section can be expressed in terms of the unpolarized structure functions $F_2 = \frac{(2M\nu - Q^2)\nu}{8\pi^2\alpha(M+\nu/2x)}(\sigma_L + \sigma_T)$ and $R = \sigma_L/\sigma_T$ as well:

$$\frac{d^2\sigma}{dxdQ^2} = \frac{\sigma_{Mott}}{E'E}\frac{\pi F_2(x,Q^2)}{x\epsilon}\frac{1+\epsilon R(x,Q^2)}{1+R(x,Q^2)}$$

The energy scales relevant to deep-inelastic lepton nucleus scattering (multi-GeV) are much higher than those relevent to the atomic nucleus (multi-MeV), thus expecting negligible influence in DIS from the surrounding nucleons. Hence, it came as a surprise that the structure function $F_2^N(x)$, which in the Quark-Parton Model represents the quark momentum distribution inside the nucleon, was found to depend on the mass number A of the atomic nucleus [2]. With $F_2^N(x)$ found to be A-dependent, it is relevant to investigate whether this dependence is the same for its longitudinal and transverse components. A possible difference in the A-dependence of σ_L and σ_T can be studied by investigating the A-dependence of R. This study involves measurements of the ratio of DIS cross section for a nucleus (σ_A) and deuterium (σ_D):

$$\frac{\sigma_A}{\sigma_D} = \frac{F_2^A}{F_2^D}\frac{1+\epsilon R_A}{1+R_A}\frac{1+R_D}{1+\epsilon R_D}$$

where R_A and R_D represent the ratio σ_L/σ_T for nucleus (A) and deuterium (D). For $\epsilon \rightarrow 1$ the cross section ratio equals the ratio of the structure functions F_2^A/F_2^D. For smaller values of ϵ the cross section ratio is equal to F_2^A/F_2^D only if $R_A = R_D$. A difference between R_A and R_D will thus introduce an ϵ-dependence of σ_A/σ_D. Hence, measurements of σ_A/σ_D as a function of ϵ can be used to extract experimental information on R_A/R_D.

The ratio of the inclusive DIS cross section off nitrogen and helium-3 with respect to deuterium from the HERMES esperiment [3] is presented in fig.2 compared to similar ratios [4]. A significant difference between HERMES data and previous data is observed for $x < 0.06$. In this domain the HERMES data for both nuclei are smaller then the NMC and E665 data and the deviation increases towards smaller values of x. At high values of x the HERMES data are in agreement with the SLAC data. Apart from the data shown in fig.2, other data show a strong reduction of σ_A/σ_D for $0.01 < x < 0.1$ and $0.05 < Q^2 < 1.5\ GeV^2$ that is similar to that of the HERMES data on ^{14}N [5]. However,

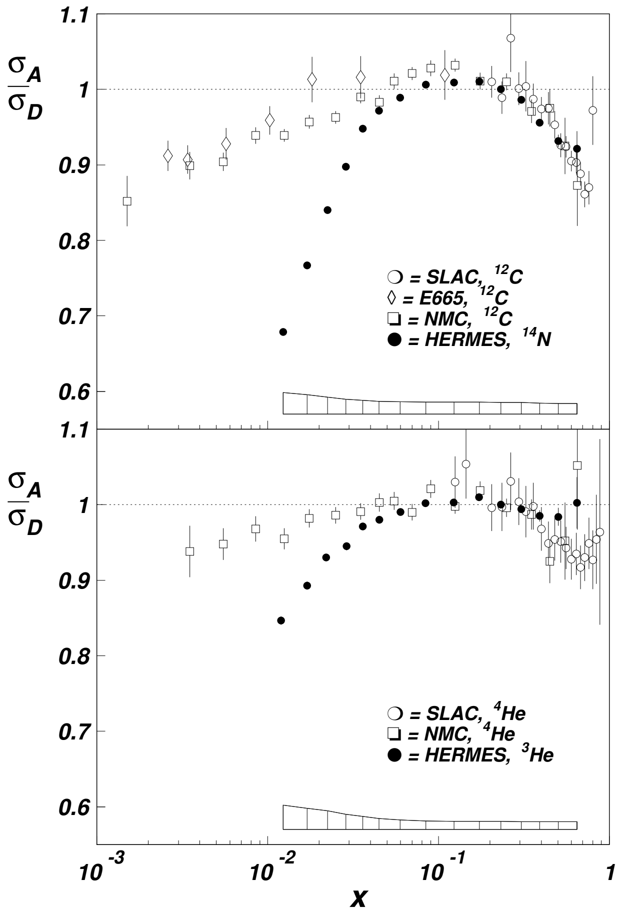

Figure 2: Ratio of inclusive DIS cross sections from nucleus (A) and deuterium (D) versus x. The systematic uncertainty of the HERMES data is given by the error band.

these data were never used to study a possible A-dependence of R, because of insufficient statistic or because of their limited kinematic coverage.

The values of F_2^A/F_2^D derived from the HERMES σ_A/σ_D data are displayed in fig. 3 for both nitrogen and helium-3. The data are in agreement with the curves representing parameterisations of F_2^A/F_2^D ratios determined using the NMC and SLAC data. The experimental uncertainties on F_2^A/F_2^D are too large to observe any systematic deviation between neighbouring nuclei.

The resulting values of R_A/R_D are shown in fig.4. The data are plotted at the average values of Q^2 for a given x-bin. The values of R_A/R_D derived from the HERMES data are considerable larger than unity for x <0.06 and Q^2 <1.5 GeV^2. In this region the deviation from unity is bigger for ^{14}N than for ^3He, as expected for a medium dependent effect. All data above Q^2=1.5 GeV^2 are seen to be consistent with unity.

The mechanism that gives rise to an enhancement of R_A with respect to R_D at low Q^2 and x do not significantly change the ratio of the structure function F_2^A/F_2^D. Since F_2^A and

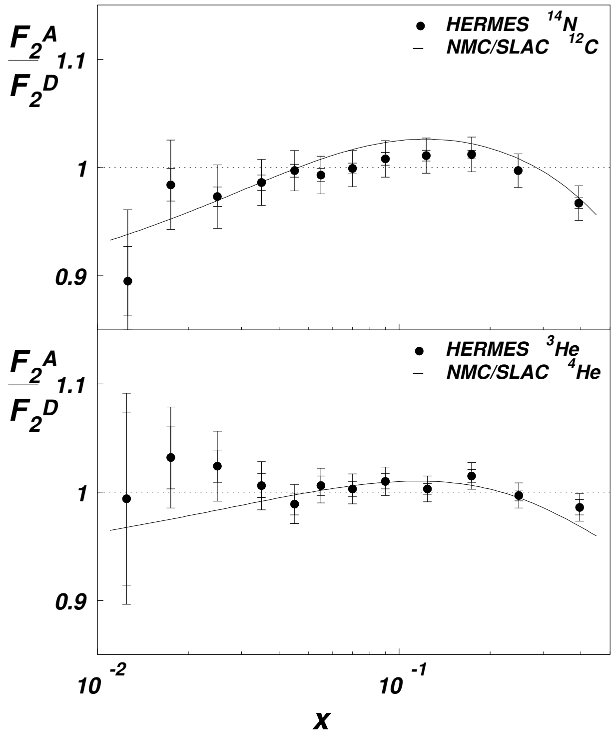

Figure 3: Ratio of the inclusive structure functions F_2^A/F_2^D. The inner error bars include the statistical uncertainty and the correlated error in R_A/R_D. The outer error bars represent the total uncertainty including the systematic uncertainty.

R_A depend differently on the longitudinal and transverse DIS cross sections, the different effects on σ_L and σ_T can be distinguished. It has been found that both an enhancement of the longitudinal response σ_L and a corresponding reduction of the transverse response σ_T are needed to explain the present data.

Possible interpretations have been suggested. Shadowing differences between σ_L and σ_T have been discussed in ref.[6, 7]. An estimate of this effect for the HERMES kinematics leads to an increase of R_A/R_D not large enough for explaining the present data. The step Q^2-dependence of the R_A/R_D also suggests an explanation in terms of a higher twist effects [8], i.e. strong quark-gluon correlations that are enhanced in the nuclear environment [9]. Recently [10] has been shown that nuclear σ, ω and π mesons can contribute coherently to enhance the electroproduction cross section on nuclei for longitudinal virtual photons at low Q^2 while depleting the cross section for transverse photons. The prospect that the mesonic fields which are responsible for nuclear binding can be confirmed as effective constituents of nuclei at small x and Q^2 is an exciting development at the interface of traditional nuclear physics and QCD.

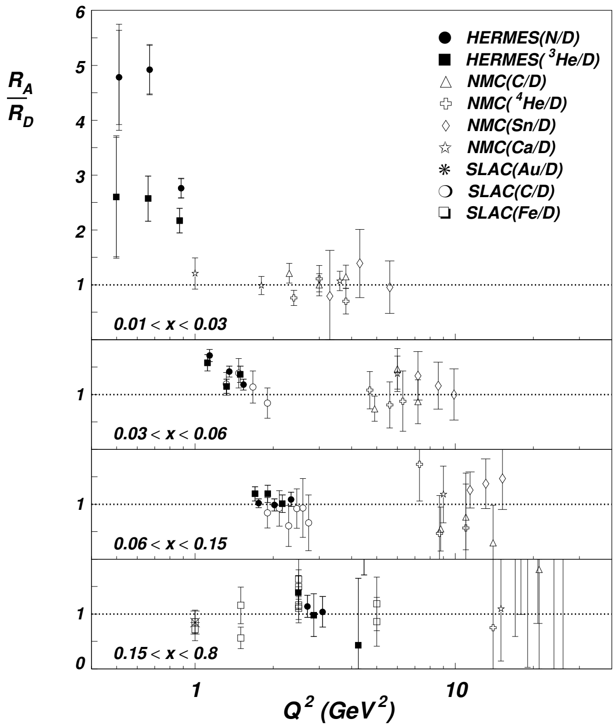

Figure 4: Ratio R_A/R_D for nucleus A and deuterium as a functions of Q^2 for four different x bins. The inner error bars include the statistical uncertainty and the correlated error in F_2^A/F_2^D. The outer error bars represent the total uncertainty including the systematic uncertainty.

4 Semi-inclusive measurements

Besides the study of the internal structure of the nucleon, deep inelastic lepton nucleus scattering offers a direct way to study the space-time development of the hadronization process, because one can use the secondary reactions of the final state particles for measuring the so-called hadron formation time (τ_f) or the corresponding hadron formation length ($l_f = c\tau_f$). In semi-inclusive DIS the struck quark will propagate over l_f before interactions with other quarks. When the quark propagation is embedded in the nuclear medium, the number of hadrons produced will depend on the interactions of the propagating quarks. Therefore the comparison of hadron distributions from DIS of leptons on different nuclei offers the best way to extract information on the formation time of the hadrons [11] [12].

At the HERMES energies (4< ν < 24 GeV) nuclear effects may be significant since l_f is of the same order of magnitude as the diameter of the target nucleus. In addition previous experiments performed at SLAC with deep-inelastic electron scattering [13], at CERN with high-energy muons by SMC [14] and with neutrinos by WA21/WA59 [15] indicate that the optimal energy range of the lepton to study hadronization dynamics with nuclei equals a few tens of GeV.

Moreover, in order to discriminate among the different models for the formation time, it is important to study the hadronization process as function of hadron species.

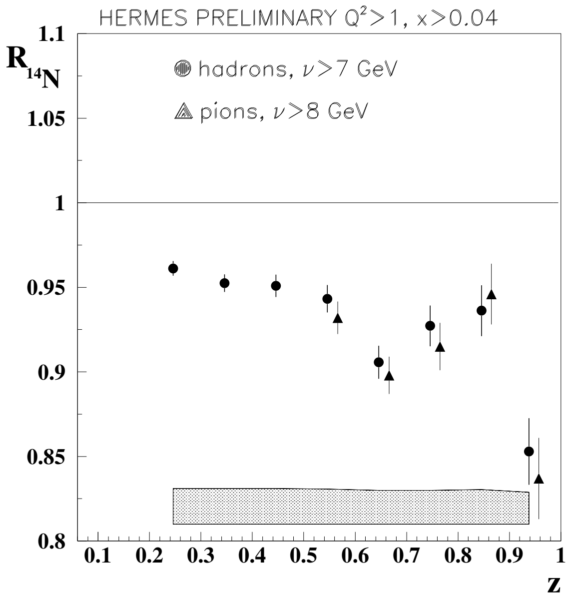

Figure 5: The attenuation ratio as function of z for charged hadrons and pions. The band represents the systematic uncertainties.

The quantity measured in the experiment is the attenuation ratio for the nitrogen $R_{^{14}N}$, defined as the ratio between the differential charged hadron multiplicity N_h normalized by the number of scattered electrons N_{DIS}, for nitrogen (N) and deuterium (D) targets:

$$R_{^{14}N} = \frac{(\frac{1}{N_{DIS}}\frac{dN_h}{dzd\nu})_N}{(\frac{1}{N_{DIS}}\frac{dN_h}{dzd\nu})_D}.$$

The preliminary attenuation ratio as function of z for charged hadrons and pions is shown in fig.5.

A significant depletion of the hadrons in the interactions with the nitrogen nucleus is seen in the whole region $0.2 < z < 1$. Pion attenuation can be studied by using the Čerenkov detector in a restricted energy region. The z behavior of the pion attenuation is similar to that of the unidentified hadron ones. It is worth noticing that the data cover the unexplored region $0.85 < z < 1$ showing a decrease of the attenuation ratio. This finding is in qualitative agreement with the predictions from different models [16, 17].

The attenuation ratio as a function of ν is shown in fig.6 for charged hadrons and pions. The ratio is observed to increase with increasing ν. This increase can be understood if at high ν the hadron formation takes place largely outside the nucleus.

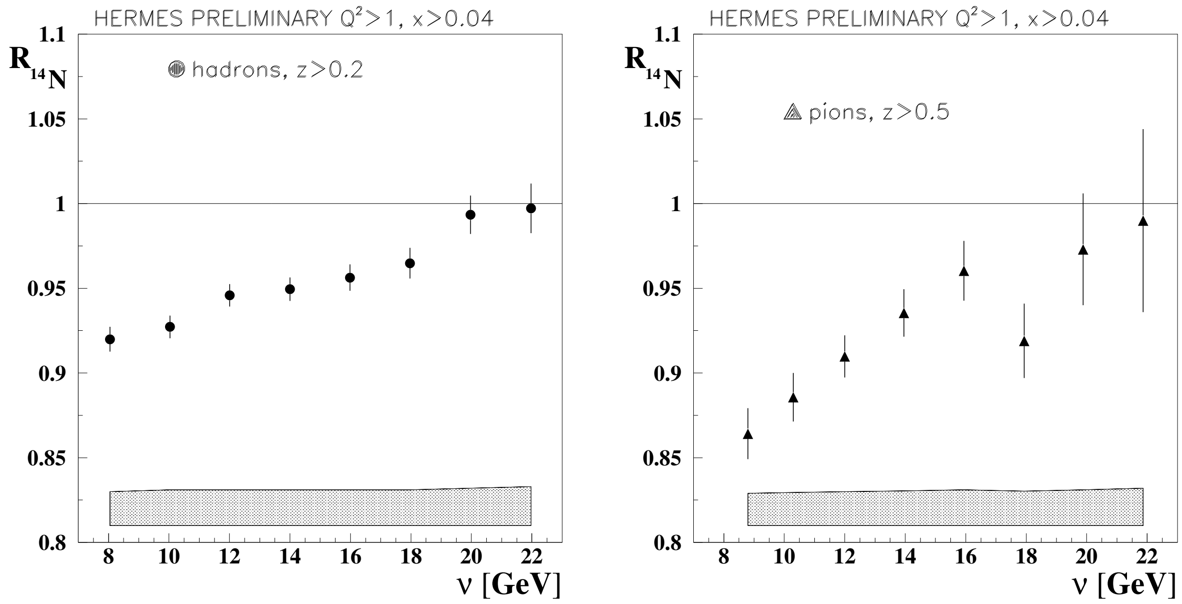

Figure 6: The attenuation ratio as function of ν for charged hadrons and pions. The band represents the systematic uncertainties.

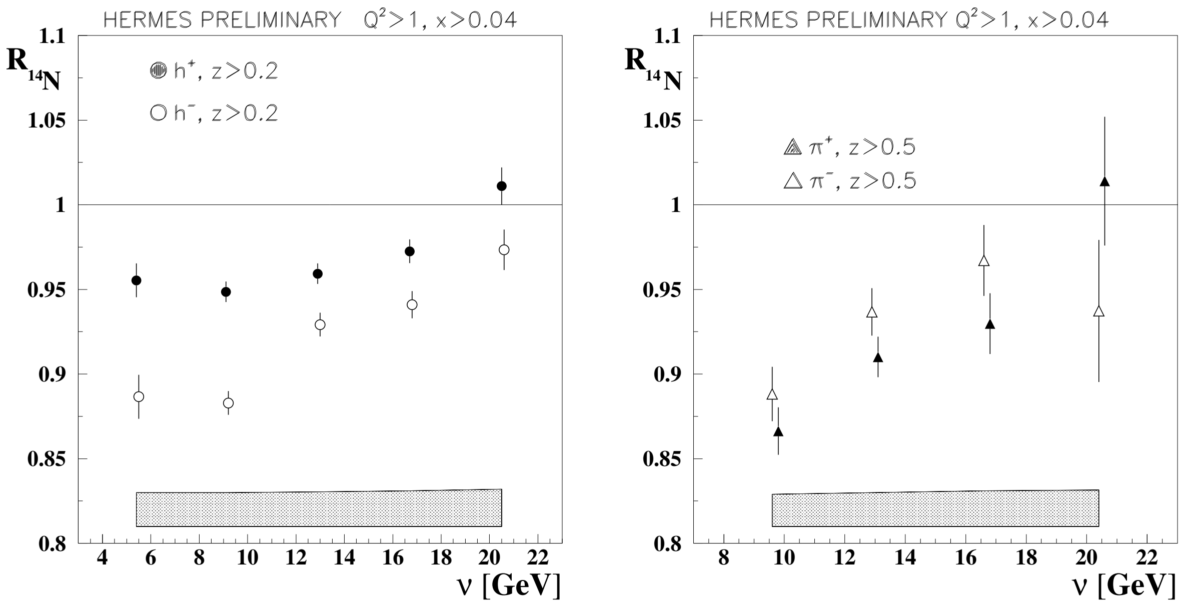

Figure 7: The attenuation ratio as function of ν for positive and negative hadrons and pions. The band represents the systematic uncertainties.

Because the hadronic mass distribution of the detected particles is very different for the positive and the negative charge samples, the hadron attenuation for the two charge states is shown in fig.7 for hadrons and pions respectively. Since the attenuation of positive and negative pions is the same within the experimental uncertainties, the difference between positive and negative hadrons must be related to the difference in attenuation of the other hadrons, mostly protons and kaons. This finding suggests that the proton attenuation is smaller with respect to the pion attenuation and therefore that the proton formation time in the hadronization process is larger than for lighter hadrons.

Additional measurements of the attenuation ratio in various heavy nuclei with pions, kaons and protons identification provided by the RICH detector are needed to clarify the issues raised by the present data. Such measurements are actually underway at HERMES.

5 Exclusive measurements

The space time evolution of a virtual quantum state such as a quark-antiquark ($q\bar{q}$) fluctuation of a photon, can be probed, in analog way to the space time evolution of the hadronization process, by studying its propagation through a perturbing medium. The $q\bar{q}$ states of mass $M_{q\bar{q}}$ propagates on a distance $l_c = 2\nu/(Q^2 + M_{q\bar{q}}^2)$, known as the "coherence length", before interacting with the nuclear medium. The interactions between the $q\bar{q}$ states and the nuclear medium can be studied at different values of l_c by varying the kinematics at which the state is produced.

In nuclear targets, photon-induced reactions can be affected by the initial state interactions (ISI) of the $q\bar{q}$ states with the nuclear medium. The ISI are maximized when l_c is large compared to the nuclear radius and the photon converts into $q\bar{q}$ before entering the nucleus thus experiencing hadronic ISI. When the l_c is small compared to the nuclear radius, the photon propagates to the point of interaction in a bare electromagnetic state and it is subject to negligible ISI.

The dependence of the ISI on l_c have been studied at HERMES in exclusive ρ_0 production, by measuring the nuclear transparency (T_A) [18]. T_A is defined as the ratio of the measured cross section (σ_A^ρ) to that expected in the absence of ISI and final state interaction (FSI) ($A\sigma_H^\rho$ where H refers to hydrogen) $T_A \equiv \sigma_A^\rho / A\sigma_H^\rho$.

The distribution of the selected events as a function of the exclusivity variable $\Delta E = (P_Y^2 - M^2)/2M$, where P_Y is the four-momentum of the of the undetected final state, is shown in fig.8a). Exclusive event, where the undetected final state consists of a nucleon recoiling without excitation, occur at $\Delta E = 0$; while non-exclusive events that involve the production of additional undetected particles appear at larger ΔE. The invariant mass $M_{\pi\pi}$ distribution for the exclusive events is shown in fig.8b). It is dominated by resonant production of the $\rho_0(770)$, with small contribution from exclusive production of non-resonant $\pi^+\pi^-$ pairs and of the $\omega(782)$ resonance.

The nuclear transparencies T_A for ^2H, ^3He and ^{14}N are shown as a function of the coherence length l_c in fig.9. Within the uncertainties the ^2H and ^3He transparencies are independent of l_c. The consistency of the deuterium transparency with unity suggests

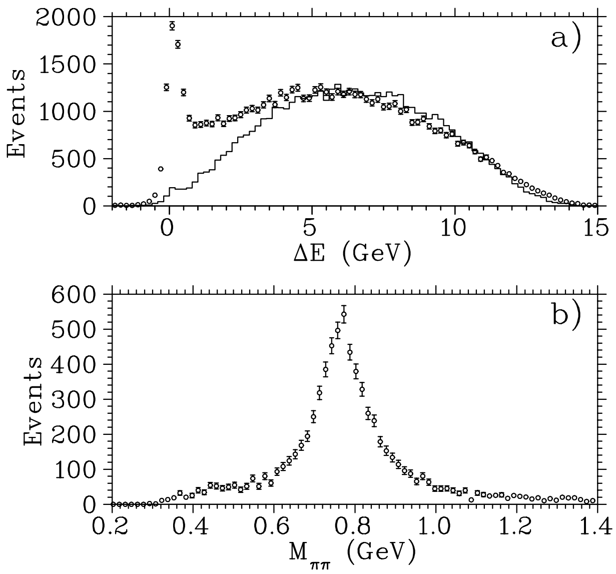

Figure 8: a) ρ_0 production events as a function of the exclusivity variable ΔE. b) Invariant mass distribution of the exclusive events.

that the ISI and FSI are small in ^2H. The nitrogen transparency exhibits the decrease due to the onset of the ISI as l_c increases. It is worth noticing that the ISI manifest at coherence length values of the order of the internucleon distance and saturate when the coherence length value is of the order of the nucleus size. Results from previous experiments [19, 20], also shown in the figure, are consistent with the HERMES data but give no indication of l_c-dependence. The $T_{^{14}N}$ and $T_{^3He}$ data are consistent with a recent prediction of the coherence length effect [21]. The consistency of the model with the data therefore suggests that when l_c is large the $q\bar{q}$ ISI are approximately as strong as the ρ_0 FSI.

The presented results provide a clear evidence of the interaction of the $q\bar{q}$ fluctuations from which the ρ_0 originates with the nuclear medium.

6 Conclusions

Nuclear effects have been studied at HERMES by performing measurements on unpolarized ^2H, ^3He and ^{14}N high density targets.

Inclusive deep inelastic scattering measurements have shown a surprisingly large suppression in the nuclear cross section at low x. This finding is explained in terms of an A-dependence of $R = \sigma_L/\sigma_T$ at low x and low Q^2. In particular, the HERMES data indicate a substantial attenuation of the σ_T and a corresponding enhancement of σ_L in nuclei and represent the first observation of a nuclear effect in the ratio of the longitudinal to transverse photoabsorption cross sections.

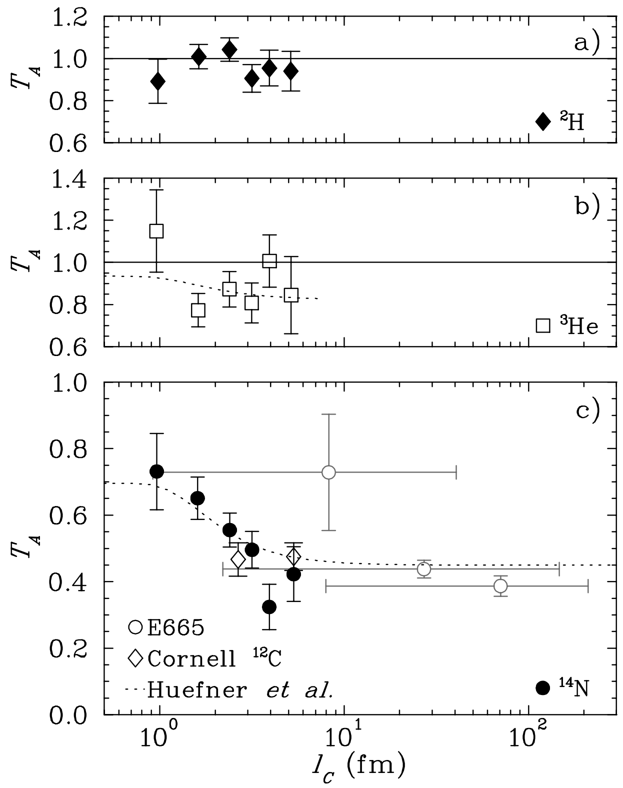

Figure 9: Nuclear transparency T_A as a function of the coherence length l_c for ^2H, ^3He and ^{14}N targets.

The nuclear attenuation of fast charged hadrons and pions, which provides informations on the time development of the hadronization process, has been measured. Preliminary results have shown a significant attenuation of fast charged hadrons and pions on ^{14}N. The attenuation was found to increase with decreasing energy transfer ν. Moreover, a possible dependence of the nuclear attenuation on the hadron mass has been for the first time evidentiated.

The study of diffractive exclusive ρ_0 production has shown a decrease of the ratio of the ^{14}N to ^1H cross sections per nucleon with increasing coherence length of the quark-antiquark fluctuations of the virtual photon. The data provide clear evidence of the interaction of the quark-antiquark fluctuations with the nuclear medium.

Further measurements on heavier nuclei, that will improve the A-dependence behavior of the aforementioned nuclear effects, are actually underway at HERMES.

References

[1] HERMES Collaboration, K. Akerstaff et al., NIM **A 417**, 230 (1998)

[2] J.J. Aubert et al. (EMC), Phys. Lett. **B 123** (1983) 275.

[3] HERMES Collaboration, K. Akerstaff et al., Phys. Lett. **B** in press, hep-ex/9910071.

[4] P.Amaudruz et al.(NMC), Nucl. Phys.**B 441** (1995) 3; M.R. Adams et al. (E665), Z. Phys. **C 67** (1995) 403; J. Gomez et al., Phys. Rev. **D 49** (1994) 4348.

[5] J. Franz et al., Z. Phys. **C 10** (1981) 105; J. Bailey et al., Nucl. Phys. **B 151** (1979) 367; J. Eickmeyer et al., Phys. Rev. Lett. **36** (1976) 289; S. Stein et al., Phys. Rev. **D 12** (1975) 1884; M.S. Goodman et al., Phys. Rev. Lett. **47** (1981) 293.

[6] N.N. Nikolaev and B.G. Zakharov, Z. Phys. **C 49** (1991) 607.

[7] V. Barone and M. Genovese, Proc. of the Workshop 1995/96 on 'Future Physics at HERA' Eds. G. Ingelman, A De Roeck and R. Klanner, DESY, 1996, p.938, hep-ph/9610206.

[8] R.K. Ellis, W.Furmanski and R. Petronzio, Nucl. Phys. **B 207** (1982) 1.

[9] S. Barshay and D. Rein, Z. Phys. **C 46** (1990) 215.

[10] G.A. Miller, S.J. Brodsky and M. Karliner hep-ph/0002156.

[11] G.V.Davidenkov, N.N.Nikolaev, Nucl. Phys. **B 135**, 333 (1978).

[12] A.Bialas, E.Bialas, Phys. Rev. **D 21**, 675 (1980).

[13] L.S. Osborne et al., Phys. Rev. Lett. **40**,25 (1978).

[14] J.Ashman et al., Z. Phys. **C 52**, 1 (1991).

[15] W. Burkort et al., Z. Phys. **C 70**, 47 (1996).

[16] B.Z.Kopeliovich, J.Nemchik and E. Predazzi, 1st ELFE Summer School on Confinement Physics Cambridge, UK; 22-28Jul 1995. Publ. in S.D. Bass and P.A.M. Guichon Ed. Frontieres, Gif-sur-Yvette, 1996 (391-395) 1995 and hep-ph/9511214

[17] J.Czyzewski, P.Sawicki, Z.Phys.**C56**, 243 (1992).

[18] HERMES collaboration K.Ackerstaff et al.,Phys. Rev. Lett.**82**, 3025 (1999).

[19] G.N. McClellan et al., Phys. Rev. Lett. **23**, 554 (1969).

[20] M.R. Adams et al., Phys. Rev. Lett. **74**, 1525 (1995).

[21] J. Hŭfner et al., Phys Lett. **B 383**, 362 (1996).